Optimization of an Autonomous Underwater Vehicle for Enhanced Stability

Devarsh Solanki[1], *Moksh* Kandhari[2], *Kutbuddin* Petrolwala[1], *Mihir* Chauhan[1*], and *Akash* Mecwan[2]
[1]Mechanical Engineering Department, School of Engineering, Institute of Technology, Nirma University, Ahmedabad, Gujarat, 382481, India
[2]Electronics and Communication Engineering Department, School of Technology, Institute of Technology, Nirma University, Ahmedabad, Gujarat, 382481, India

Abstract. AUVs have essential applications in oceanic investigations, environmental characterization, and subsea surveys where accuracy in positioning and stability for navigation is challenging. AUV proposed in the present work addresses these issues by utilizing a novel thruster configuration and an underwater adaptive control scheme for stability. The thruster layout helps the AUV to maneuverers in six degrees of freedom. The system uses an Adaptive PID controller, that adjusts the control parameters in real-time, which allows for a smooth and efficient running of the process as the environment changes. The AUV integrates sensor fusion, adaptive control and propulsion design. This work demonstrates a feasible and robust approach suitable for future AUV missions which requiring precision, versatility and reliability.

1 Introduction

The stability of the autonomous underwater vehicle (AUV) is a key factor for its efficient working especially when performing high precision operation. Such applications, like deploying acoustic beacons for location marking, the recovery of sensitive items such as flight data recorders or even performing delicate rescue operations with robotic manipulators require micro-scale adjustments and can be considered precision work. Ensuring stability of the vehicle against underwater currents and other disturbances is critical in delivering the safety, accuracy, and success of such complex missions. Prior works focused majorly on an AUV [1] with autonomous navigation[2], obstacle avoidance[3], and the precise placement or retrieval of objects using acoustic localisation[4]. These particular target applications naturally required the vehicle to be very stable in orientation and in position in order to provide and perform micro-adjustments.

Recent work in AUV stability and control emphasises full 6-DOF modelling and energy-efficient design. For example, Makam et al.[5] develop a 6-DOF hydrodynamic model of an AUV and analyse robust PID and sliding-mode controllers under uncertainties. In a similar vein, Lin et al.[6] , use a digital twin and 6-DOF equations to train deep-RL controllers for docking, reporting approximately 25% less depth oscillation than conventional methods. On

[1]Corresponding author: mihir.chauhan@nirmauni.ac.in

the propulsion side, Deng L[7], design an 8-thruster layout and a QP-based allocation algorithm; their simulations show notably lower power draw and better efficiency than standard pseudo-inverse allocation. Finally, Qi et al.[8] introduce an event-triggered sliding-mode depth controller that cuts unnecessary updates to save energy, achieving longer mission endurance. Nevertheless, due to the vehicle's instability, its missions could not be fulfilled as planned.

A detailed investigation revealed a number of causes for the instability. These included a less symmetric thruster arrangement, which produced a nonlinear pitch response. As well, problems like incorrect weight distribution, a non-symmetric horizontal plan design, sensor noise etc. The vehicle's performance was also limited by an inferior control system and absence of important feedback from critical instruments, such as a Doppler Velocity Logger (DVL).

To overcome these important deficiencies and improve the performance of the vehicle, a two-stage optimization approach in the mission level is proposed in this paper. The work concentrated on mechanical modifications (thruster layout, buoyancy distribution) and control architecture (adaptive PID controller in conjunction with feedback from a sensor fusion algorithm). This paper presents the analysis of such instabilities, and the following design changes that led to the increased holding stability required for the high precision work in underwater.

2 Structural optimization

There were comprehensive mechanical changes made between versions of the AUV to eliminate the instability of the previous design. The main change was the thruster configuration, which was redesigned to maximise the force vectors and to remove destabilising moments that have previously resulted in vehicle control problems. The chassis of the AUV was redesigned to be symmetrical along all two planes. This geometric symmetry is essential for predictable dynamics, since control inputs do not cause unintended cross-coupled motions. This structural modification was accompanied by a new stability method. The centre of mass is controlled by using dead weights instead of controlling the centre of buoyancy using foams. This weight distribution simplifies the vehicle’s dynamics while performing rotational motions. This combination of an even thruster arrangement, axial symmetry and centralized mass forms a new baseline in AUV static and dynamic stability.

2.1 Thruster configuration of the AUV

Analysis is performed on different thruster configurations for comparing vehicle’s dynamic performance based upon parameters such as vehicle’s manoeuvrability energy efficiency and system reliability. The study considered the conventional configuration as a standard for baseline performance. This configuration has four dedicated vertical thrusters to control heave, roll, and pitch, alongside four 45° vectored horizontal thrusters at the corners responsible for surge, sway, and yaw.

The conventional configuration is countered with an eight-thruster configuration (as shown in **Fig. 1**), where all thrusters produce thrust in three directions and all thrusters contribute in all 6 DOFs. In this proposed model, each thruster is uniformly inclined at 45° from the surge axis and 60° from both the heave and sway axes as shown in Fig. **1**(d). This proposed configuration is distinct from the other similar arrangement, where thrusters are typically arranged such that to provide equal thrust along all principal axes.

The core of the proposed methodology involves analysing the dynamic response and control of both the conventional (in-plane thruster arrangement with single axis inclination) and proposed models under various parameters.

2.1 Thrust analyses

A quantitative analysis of thrust components reveals a clear and definitive advantage for the modified 3D vectored configuration when compared to the baseline model.

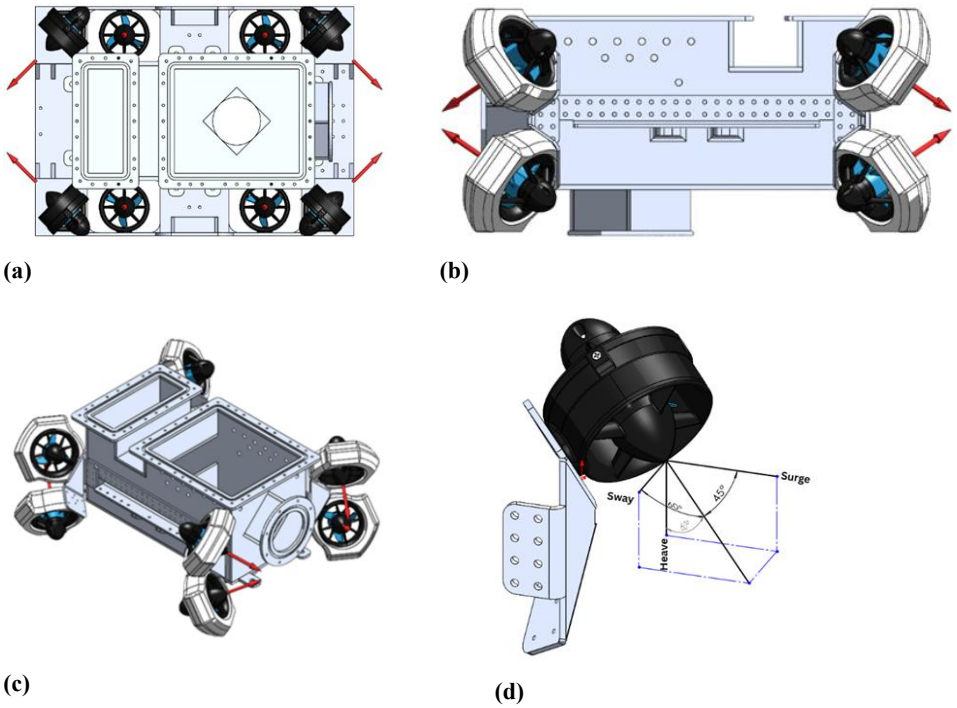

Fig. 1. Thruster configuration (a) Top view, (b) left-side view, (c) Isometric view, (d) Angle made by Thruster Line of Action with different axis

The baseline conventional configuration represents separate set of thrusters for surge/sway and heave axes, which is its primary limitation. It comprises, four dedicated vertical thrusters providing 100% of maximum thrust force (T) to the heave-axis and, four lateral thrusters at 45° (see **Fig. 1 (a), (b), (c)**), providing 70.7% T (as per equation (1)) to both the surge and sway axes. This creates inefficient force distribution. Different set of thrusters produce thrust in different axes, half of thrusters only operate in surge, sway and yaw operations and other operate heave, pitch and roll. Therefore, while manoeuvring in a single axis, half of the thrusters do not contribute any thrust, hence there is significant loss in potential thrust. Thrusters' force (T) is distributed as:

$$\textit{Surge axis force} = T.cos(45°) = 0.707T \quad (1)$$
$$\textit{Sway axis force} = T.cos(45°) = 0.707T$$
$$\textit{Heave axis force} = T$$

In the proposed configuration, all eight thrusters contribute thrust in all degree of freedom. The thrusters are thrusters are angled at 45° from the surge axis, and 60° from the sway axis, and 60° from the heave axis (see **Fig. 1**. (d)). The thrust force generated is broken down in three components and the thrusts' force (T) distribution is given as:

$$\textit{Surge axis force} = T.cos(45°) = 0.707T \quad (2)$$
$$\textit{Sway axis force} = T.cos(60°) = 0.5T$$
$$\textit{Heave axis force} = T.cos(60°) = 0.5T$$

Table 1 Thrust force comparison

Direction	Thrust Force per Thruster		Net Thrust Force	
	Conventional	Proposed	Conventional	Proposed
Surge	0.707T	0.707T	2.828T	5.656T
Sway	0.707T	0.5T	2.828T	4T
Heave	T	0.5T	4T	4T

There is no performance loss in the heave axis. The total heave force generated by the conventional configuration is equal to heave force generated in proposed configuration. The proposed configuration has larger thrust force generated in surge and sway operations. The maximum surge force is double in the proposed configuration as compared to conventional configuration. Additionally, the thrust force generated in sway axis is 28.3% greater than that of the conventional configuration. Therefore, the proposed configuration is more efficient and powerful design when compared to conventional configuration.

2.2 Energy efficiency

A key advantage of the proposed configuration is its better power efficiency during surge manoeuvres, particularly at typical cruising speeds. This is proven by the non-linear relationship between thrust and power shown in the thruster performance graph (Figure 2(a)). For example, a target net surge thrust of 4.0Kgf is required for cruising.

In the conventional configuration, to achieve thrust force of 4.0Kgf, each of the four active surge thrusters must produce 1.0Kgf in surge direction. Thus $\sqrt{2}$Kgf thrust force per thruster. According to the graph, $\sqrt{2}$Kgf of thrust requires approximately 44W of power per thruster.

In the proposed configuration, to achieve the same thrust force of 4.0Kgf, the load is spread across eight thrusters, each needing to produce only 0.5Kgf. Thus only $1/\sqrt{2}$Kgf per thruster. According to the graph, $1/\sqrt{2}$Kgf of thrust requires only 15W. Using 15W as a conservative estimate, the total power consumed in both cases are shown in Table 2. Additionally, the thrust efficiency which is defined as the thrust per unit power consumption in both the configuration is also shown in **Table 2**.

Table 2 Power consumption comparison

Configuration	Power per thruster	No. of thrusters	Total power	Thrust efficiency
Conventional	44 W	4	176 W	0.22 N/W
Proposed	15 W	8	120 W	0.32 N/W

This calculation demonstrates that to achieve the same 4.0Kgf of forward thrust, the proposed configuration is approximately 47% more power-efficient. This improvement in efficiency is simply the result of running more thrusters at a lower, more efficient point on their power curve, and it is a big plus. If we apply such an efficiency consideration to other directions, as for depth control, then we are pushed further into the design's trade-off. Maintaining depth consumes low power in both configurations because the AUV is built to be nearly neutrally buoyant. Thus, keeping a stable depth requires very less energy. This is compounded by the fact that depth changes are not a part of AUV operations AUV operations typically do not involve constant, active depth variations. Sway and yaw manoeuvres trade-off must also be considered. In these directions, the proposed configuration is more power

consuming for the amount of thrust it produces, this is an unavoidable consequence of this configuration.

The reduction in efficiency is a calculated sacrifice for a significantly greater maximum thrust and stability. The proposed design intentionally locates the thrusters at a large distance from the AUV's centre of gravity. This placement creates a large moment arm, is a very important quantity in rotational mechanics. Because of this greater leverage, the AUV is able to develop great moment with very little thruster output. Therefore, the power needed to control the orientation and to maintain a steady heading is small, which guarantee the vehicle stability and manoeuvrability.

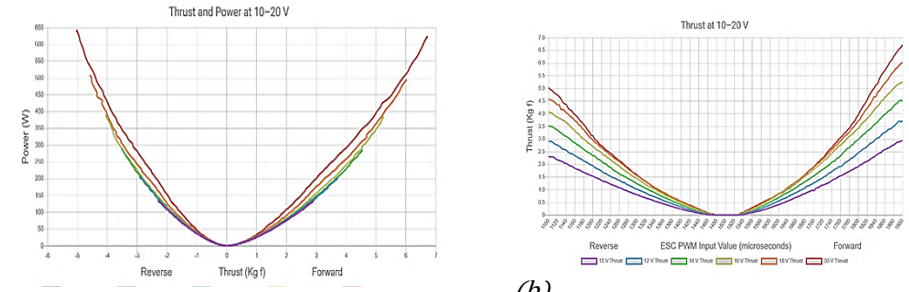

(a) *(b)*

Figure 2 Thruster characteristics (a) Power vs Thrust curve*[10]* (b) Thrust vs PWM curve*[10]*

2.3 Thrust force alignment

The redesigned arrangement of the AUV thrusters improves stability as the thrust force vectors are oriented along the AUV's centre plane in the surge direction, which decreases the coupling of the surge–pitch motions, and enables to achieve fine and dependable controls through the adjustable and symmetric mounting system.

Standard thruster arrangement, thrusters' lines of action are the farthest from the vehicle's central line. This offset alignment means that forward thrust produces a moment about the AUV, tending to pitch the AUV forward. The effect of this unintended coupling of surge and pitch motions was the major contributor of instability.

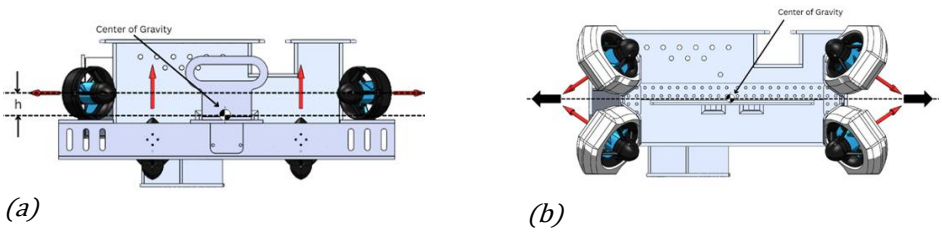

(a) *(b)*

Figure 3 (a) Standard thruster configuration, (b) proposed thruster configuration.

The proposed design solves the problem perfectly, as can be evident from **Figure 3(b)** where the new design exhibits a high degree of symmetry with the thruster brackets nearly collinear with the horizontal axis that intersects the centre of the machine. This design could be further modified by means of adjustment mounts. This built-in fault the thrusters' line of action can be finely tuned in the area of the thrust force vector that is closest to the centre of gravity. In doing so this effectively takes away the pitch moment of the vehicle allowing for stable manoeuvring.

2.4 Dynamic stability

The static stability of the proposed design was maximized at the expense of the dynamic stability. It is standard practice to compensate for any offset in the vehicle's Centre of Mass (CoM) by adding buoyant material (foam, floatation, etc.). This brings the Centre of Buoyancy (CoB), into a vertical line with the CoM, which produces a passive restoring moment that can keep the vehicle stable at rest. This strategy achieves static stability, but imposes a large spatial separation between the centre of mass (CoM) and the body of the device. It is this off-centre displacement that is a major source of unwanted moments in rotary manoeuvring. This tension in design leads to a dynamically unstable vehicle that requires constant thruster compensation to maintain an equilibrium trajectory. The present method overcomes this limitation by using full stability method. Weights and buoyancy materials (foam, floats, etc.) are no longer post-design additions but key elements built into the vehicle frame. The whole engineering challenge is creating a method to accurately co-locate the Centre of Mass and Centre of Buoyancy so that they lie on the same vertical line. This vertical shaft should lie at the centre of the machine. Axis pointing also improves stability as buoyant force can generate a restoring torque when instability occurs. Therefore, the design cancels out the major source of unwanted moments and ensures the robot to be inherently dynamically stable. This alignment is done in conjunction with the placement of components to ensure the vehicle is statically stable and has sufficient net positive buoyancy to be recovered. Such a simplification of a physical AUV dynamics is an essential design step to avoid unintended hydrodynamics and reduces drastically the compensation effort on the control system.

2.5 Hydrodynamic flow and drag reduction

Hydrodynamic pressure drag was a major design issue for the baseline and the proposed configurations. Both sets of thrusters are designed to minimize this drag by pulling water from the front and pushing it out the back. This propulsive flow is designed to “compensate” the low-pressure wake that would normally develop underneath the auv, which reduces the pressure difference over the hull and the pressure drag[11]. A distinct benefit of the designated configuration is that it has more scope for this effect. In this configuration which is being proposed all 8 thrusters are involved in this longitudinal flow during a backward movement. That combined effect is supposed to create a much stronger boost in the flow-through effect with the result of a lower drag pressure profile than the base line case where only four thrusters were involved. Secondly, the older frame's geometry was non-symmetric which automatically resulted in flow imbalance around the hull. This asymmetry induced a lot of unwanted turbulence. More importantly, it caused different drag forces to act on different parts of the vehicle, producing unwanted torques that continuously tried to yaw (turn left or right) and pitch (nose up and down) the auv away from its path of travel. On the other hand, the very symmetrical frame of the proposed design rectifies the problem. This arrangement allows for a much more consistent and better flow velocity field on the hull surface. This greater homogeneity of hydrodynamic flow contributes a great deal to the auv’s markedly superior dynamic stability as it causes its trajectory to be much more predictable.

3 Thrust control PID optimisation of AUV

The improvement of the physical architecture of the AUV is substantial, but the development of the necessary advanced control to provide the appropriate levels of stability and accuracy is also very challenging. While somewhat conservative for a number of linear systems,

decade provides a functional starting point. The conventional Proportional-Integral-Derivative (PID) control algorithm, given by:

$$\tau_0 = K_p(t)e(t) + K_i(t)\int e(t)dt + K_d(t)\dot{e}(t) \quad (3)$$

The thruster based PID is selected against the speed controller based PID algorithm which is conventionally used. Control of an underwater vehicle differs from basic PID control operations as AUV requires control over 6DOF in an uncertain and turbulent underwater environment that has strong external perturbations. Hence a thrust based PID control scheme is proposed, as forces produced by propellers are correlated with the dynamics of the machine. While the speed based control scheme affects the dynamics of the machine in a non-linear manner, as there is no functional correlation of PWM input and thrust. While providing more predictive control, this control algorithm also helps in eliminating the "dead zones" (PWM range where propellers produce no thrust) of the propellers. The thrusters' PWM vs Thrust (**Figure 2**) shows that at the PWM range 1450 to 1540, there is no thrust generated by the thruster. If the PWM PID gives an output in this range, there will be no correction in the error. The thrust based PID gives output in thrust required, then the PWM is found out using the PWM vs Thrust curve. This value of PWM is given to the propeller. Thus, the thrust based PID controller along with anti-windup, with user defined-logic based on specific AUV hydrodynamic and inertia characteristics offers more predictive and higher degree of stability. With this in mind, it was recognized that a customized control scheme was necessary - one which could take into account the specific dynamics of the vehicle and maximize the operational effectiveness through such an optimization. In response to these issues, a novel control scheme, called Proactive Adaptive PID Controller, is put forward.

3.1 Proactive adaptive PID gain scheduling

One of the key challenges to realizing any PID-based controller on real hardware is salted by nonlinearities such as Actuator Saturation. Saturation happens when the command value computed by the controller is bigger than the physical limit of the thrusters' outputs at either ends of scale of magnitude limits. When coupled with the controller's integral term, this physical constraint becomes a drastic source of instability, resulting in the phenomenon known as Integral Windup. If a lingering error is present while the actuators are saturated, the integral term, oblivious to the saturation, will persist in accumulating to a harmful, unproductive magnitude. The wound-up condition is very destabilizing as it prevents the system from attaining a steady stable operating point often generating large overshoots and sustained oscillations even after the error has been eliminated. As counter measure a well-known anti-windup technique, integral clamping, is adopted. This process will stop the integral accumulation conditionally in the meanwhile keep the integral from winding up. The clamping logic is activated only if two conditions hold true simultaneously: (1) the controller output has been saturated and (2) the sign of the error is toward the integrand, i.e., it will increase the magnitude of the integral term.

This means that the integral term is always a realistic, bounded and computable history of the error, which allows for fast system settling and good steady-state stability. The disadvantages of actuator saturation are immense in a multi-DOF AUV. This results in experiencing complicated cross-coupling motions. A fundamental difficulty emerges when a command has to be exerted along a multi-DOFs at once, say a pure rotational command that requests precision opposing thruster forces to keep away any translational movement.

If any of the propellers needed for the manoeuvre saturate in the course of performing its primary function, it may no longer have the capability to generate the necessary oppositional thrust that is required for the secondary purpose. This creates a force vector that is "off-

balance," which leads to the very translational drift during an orientation command that the controller is intended to mitigate.

As a solution to this, a supervisory thruster allocation logic is proposed whose design is guided from the outset by the aim of preserving the proportion of the desired force/torque vector. This allocator is executed dynamically and examines first if any thruster in the system is saturated by the current command. When this saturation happens, the limiting action is performed, that is, the allocator computes what maximum factor can be applied to the entire desired force/torque vector proportionality before any thruster reaches its saturation limit. This scale factor is uniformly applied to saturate all thrusters including the non-saturated ones."

The direction and the force/torque ratio of the force and torque vector are exactly preserved, only the norm is scaled down to the physically achievable norm of the control action, since the control action is normalized. This ensures that no undesired (imbalanced) force vector is generated, which may otherwise cause translational drifts while spinning.

To formally describe the adaptive mechanism, the controller gains are updated in real time based on the instantaneous tracking error. The tracking error is defined as the difference between the desired reference state $r(t)$ and the measured system output $y(t)$.

$$e(t) = r(t) - y(t) \quad (4)$$

The proportional, integral, and derivative gains are adjusted online using predefined adaptation laws:

$$K_p(t+1) = K_p + \alpha e(t)\dot{e}(t) \quad (5)$$
$$K_i(t+1) = K_i + \beta e(t) \quad (6)$$
$$K_d(t+1) = K_d + \gamma \dot{e}(t) \quad (7)$$

In these equations α, β, and γ are adaptation coefficients that control the rate at which the controller gains are modified. These adaptation rules enable the controller gains to increase when the tracking error becomes large and gradually settle as the system approaches the desired operating condition. Consequently, the controller can automatically adjust to disturbances and nonlinearities present in the system. From a stability standpoint, the formulation of the adaptation laws ensures that the controller parameters remain within finite limits. When disturbances are bounded and the adaptation coefficients are selected appropriately, the tracking error progressively converges toward zero. This behaviour helps maintain the closed-loop stability of the AUV's motion control.

3.2 Thrust based control command

In standard control practice, the output of a PID controller is often a direct Pulse-Width Modulation (PWM) signal. This signal is passed then to the motor controller of the thruster. Yet, such a method results in large inefficiencies and non-linearities which impair the control performances. The basic issue is that the mapping between the applied PWM signal and the actual thrust force of a propeller is strongly nonlinear. In addition, it is the thrust, not the PWM, that directly determines the dynamic behavior of the AUV. Calculating PID commands in the PWM domain ends up being an exercise in futility, since it's trying to control the vehicle's dynamics with a value that is one step removed and is not linearly related to the forces and torques that actually influence the vehicle. To overcome this weakness, a control structure is derived in the thrust domain. The PID controller logic is tuned to produce the exact thrust needed to correct a given error in the AUV state. This desired thrust command is fed into a separate conversion block. This module applies a predefined thrust-to-PWM map from an empirical "PWM vs. Thrust" (see **Figure 2(d)**) for each thruster This work instructions.

This function effectively works as a look up table, which invert the nonlinear thruster dynamics, that is the function calculates the PWM value needed to revolve the thruster at the speed required t the exact thrust that was commanded by the PID. A critical flaw in direct PWM control is the thruster "dead zone". As illustrated in a typical thruster calibration graph (see), propellers produce zero thrust until the applied PWM signal reaches a certain minimum threshold.

This presents a major problem for a conventional PID controller. When attempting to correct a very small, persistent error, the controller might output a small PWM command that falls entirely within this dead zone. The result is that no control action occurs and the error persists. The thrust-based architecture completely eliminates this problem. When the controller commands a small but non-zero thrust, the conversion module looks up the correct PWM value to achieve this. Based on the calibration graph, this value will be above the dead zone threshold. This ensures that any non-zero thrust command from the PID results in an immediate and proportional physical response from the thruster.

This capability is critically helpful, as it prevents the micro-errors and low-amplitude oscillations that are common when a controller is fighting against a hardware dead zone. In dynamic conditions, these small errors can accumulate producing undesired translational or rotational drifts that the control system is designed to prevent, thereby enhancing fine-scale stability.

3.3 Proportional-derivative clamping

In order to obtain a fast and high bandwidth control for the AUV damping motion. It is needed to employ an aggressive derivative term (K_d). Derivative action, being predictive control will oppose aggressive variation of error and brakes down the system when it is close to the setpoint. This helps the system to settle rapidly.

However, this technique is extremely sensitive to noise. The nature of the derivative term tends to accentuate any high frequency and non-deterministic noise in the error signal. This excitation generates a noisy and unstable control thrust output. This phenomenon can destabilise the vehicle, it may overshoot, and ironically it can keep the system from settling. Although conventional noise filters were applied to the error signal, they were not adequate to eliminate the compromise completely. A more robust approach is necessary to retain the high damping advantages of a large K_d but mitigate its destabilizing character. To that end, a special clamping technique is applied on the derivative output itself. The basic idea of the method is to adaptively limit the derivative term magnitude ($K_d * \frac{d(e)}{dt}$) considering proportional term magnitude ($K_p * e$). The clamping value is evolving with the proportional term and regulated by the parameter K_c. The proportional and the (unfiltered) derivative terms are ($K_p * e$) and ($K_d * \frac{d(e)}{dt}$) respectively. A dynamic limit for the derivative term is computed as $K_c * (K_p * e)$, while the final derivative output is clamped, to this dynamic limit and computed as,

$$\text{Final derivative output} = \text{Max}\left[-K_c * (K_p * e), \text{Min}\left\{(K_d * \frac{d(e)}{dt}), K_c * (K_p * e)\right\}\right] \quad (8)$$

This has the effect of relaxing the derivative action. When the error (e) is large, the Derivative Limit is also large, so the derivative can be aggressive and help to control the system. Importantly, the Derivative Limit also decreases as the error goes to zero to reduce the derivative term's overreaction of noise and to prevent it from causing oscillations in the neighbourhood of setpoint. This proportional-derivative clamping strategy yields two important, synergistic benefits: It permits the use of much larger K_d values than would

initially be stable, thereby allowing for maximal oscillation damping without the concern of noise-induced destructive oscillations. And with a robust and stable derivative term now controlling the system's approach, higher K_p values can also be used to obtain faster responses, without the usual concerns about overshooting. The net effect is a substantial reduction in a vehicle's aligning time. This improvement is especially important for operation mode where high fidelity control is needed, e.g. small micro moving at manipulation process like object retrieval under the arm, or accurate payload dropping, etc., which require the smallest settled time with no overshoot.

4 Conclusion

Two objections are weight distribution, buoyancy alignment and hydrodynamic design for the static and dynamic stability. A novel thruster configuration, which provides full six-degree-of-freedom control and is optimised for thrust efficiency and manoeuvrability, is introduced allowing accurate motion control even in turbulent underwater environment. An adaptive PID controller with fusion of the sensor data from sonars and visual sensors contributed to the dynamic stability and reactivity as it modifies the control parameters on real-time. In general, the proposed optimized AUV do better performance in stability, flexibility and energy cost, which enable it applicable for various underwater tasks. This work paves the way for developments of intelligent, adaptive, and autonomously underwater systems, which can perform decorative tasks with higher precision and reliability.

Reference

1. K. K. S. Arun, K. Jagadeesh, and M. Santhakumar, Ocean Engineering **288**, 116 (2023)
2. Blue Robotics Inc, Blue Robotics Inc (2025)
3. A. Hussain, L. Shuaiyong, T. Hussain, W. A. Razaz, and H. A. Amal, Kuwait Journal of Science **53**, 100506 (2026)
4. K. Bhatt, N. N. Panchal, I. L. Saijwal, A. Chauhan, S. Gondaliya, A. Mecwan, and M. Chauhan, International Journal of Satellite Communication & Remote Sensing **8**, 1 (2022)
5. R. Makam, P. Mane, S. Sundaram, and P. B. Sujit, (2024)
6. Y. H. Lin, P. C. Chuang, and J. Y. T. Huang, Computers, Materials and Continua **84**, 4907 (2025)
7. L. Deng and J. Tao, Mathematics **13**, (2025)
8. Y. Qi, X. Wu, G. Zhang, and Y. Sun, J. Mar. Sci. Eng. **10**, (2022)
9. Y. Kwon, D.-H. Kim, J. Seo, and H. Chung, J. Mar. Sci. Eng. **13**, 10 (2025)
10. P. Ridao, M. Carreras, D. Ribas, P. J. Sanz, and G. Oliver, Annu. Rev. Control **40**, 227 (2025)
11. F. Zhang, W. Cao, J. Gao, S. Liu, C. Li, K. Song, and H. Wang, J. Mar. Sci. Eng. **12**, 1991 (2014)